20. Khare, P. B., Studies in *Pteris vittata* L. complex. *Indian Fern J.*, 1995, **12**, 43–50.
21. Fraser-Jenkins, C. R., *New Species Syndrome in Indian Pteridology and the Ferns of Nepal*, International Book Distributors, Dehradun, India, 1997.
22. Wang, Z.-R., A preliminary study on cytology of Chinese *Pteris*. *Acta Phytotax. Sin.*, 1989, **27**, 421–438.
23. Rabe, E. W. and Haufler, C. H., Incipient polyploid speciation in the maidenhair fern (*Adiantum pedatum*; Adiantaceae). *Am. J. Bot.*, 1992, **79**, 701–707.
24. Lande, R., Extinction risk from anthropogenic, ecological and genetic factors. In *Genetics and Extinction of Species* (eds Landweber, L. A. and Dobson, A. P.), Princeton University Press, Princeton, NJ, 1999, pp. 1–22.
25. Kang, M., Ye, Q. and Huang, H., Genetic consequence of restricted habitat and population decline in endangered *Isoetes sinensis* (Isoetaceae). *Ann. Bot.*, 2005, **96**, 1265–1274.
26. Mehra, P. N., Chromosome numbers in Himalayan ferns. *Res. Bull. (N. S.) Panjab Univ.*, 1961, **12**, 139–164.
27. Sankariammal, L. S. and Bhavanandan, K. V., Cytological studies on some members of Pteridaceae (sensu Copeland) from south India. *Indian Fern J.*, 1991, **8**, 87–92.
28. Mehra, P. N. and Verma, S. C., Cytotaxonomic observations on some West Himalayan Pteridaceae. *Caryologia*, 1960, **13**, 619–650.
29. Manton, I. and Sledge, W. A., Observations on the cytology and taxonomy of the pteridophytic flora of Ceylon. *Philos. Trans. R. Soc. London, Ser. B*, 1954, **238**, 127–185.
30. Verma, S. C. and Khullar, S. P., Cytology of some west Himalayan Adiantaceae (sensu Alston) with taxonomic comments. *Caryologia*, 1965, **18**, 85–106.
31. Mahabale, T. S. and Kamble, S. Y., Cytology of ferns and other pteridophytes of Western India. *Proc. Indian Nat. Sci. Acad.*, 1981, **47**, 260–278.
32. Fabbri, F., Primo supplemento alle tavole chromosomiche delle pteridophyta Di Alberto Chiarugi. *Caryologia*, 1963, **16**, 237–335.
33. Irudayaraj, V. and Manickam, V. S., SOCGI plant chromosome number reports IV. *J. Cytol. Genet.*, 1987, **22**, 156–161.
34. Wagner Jr, W. H., A biosystematic survey of United States ferns, a preliminary abstract. *Am. Fern J.*, 1963, **53**, 1–16.
35. Punetha, N., Cytological observations on ferns of Kumaon (N. W. Himalayas). In *Plant Science Research in India* (eds Trivedi, M. L., Gill, B. S. and Saini, S. S.), Today and Tomorrow's Printers and Publishers, New Delhi, 1989, pp. 459–465.
36. Mitui, K., Chromosomes and speciation in Ferns. *Sci. Rep. Tokyo Kyoiku Daigaku, Ser. B*, 1968, **13**, 285–333.
37. Tsai, J.-L. and Shieh, W.-C., A cytotaxonomic survey of the pteridophyta in Taiwan (1): Material collection and chromosome observations. *J. Sci. Engin.*, 1983, **20**, 137–159.
38. Roy, R. P., Sinha, B. M. B. and Sakya, A. R., Cytology of some ferns of Kathmandu valley. *Brit. Fern. Gaz.*, 1971, **10**, 193–199.
39. Takamiya, M., *Index to Chromosomes of Japanese Pteridophyta (1910–1996)*, Japan Pteridological Society, Tokyo, 1996.
40. Nakato, N. and Kato, M., Chromosome numbers of ten species of ferns from Guam, South Mariana Islands. *Acta Phytotax. Geobot.*, 2001, **52**, 125–133.

ACKNOWLEDGEMENTS. This work was carried out under support from the Department of Biotechnology, Government of India, New Delhi in the form of a Grant-in-Aid project. We thank Director, NBRI for facilities. We also acknowledge the St Xavier's College at Tirunelveli (Tamil Nadu), Botanical Survey of India at Coimbatore (Tamil Nadu), Kolkata (West Bengal), Gangtok (Sikkim) and Itanagar (Arunachal Pradesh); and Department of Botany, Calicut University, Calicut, Kerala, for help with plant material.

Received 31 May 2006; revised accepted 22 January 2007

Assessment of land subsidence phenomenon in Kolkata city, India using satellite-based D-InSAR technique

R. S. Chatterjee[1,*], P. S. Roy[2], V. K. Dadhwal[1], R. C. Lakhera[1], T. X. Quang[3] and R. Saha[4]

[1]Indian Institute of Remote Sensing, National Remote Sensing Agency, Dehradun 248 001, India
[2]National Remote Sensing Agency, Department of Space, Hyderabad 500 037, India
[3]Hanoi University of Mining and Geology, Vietnam
[4]West Bengal State Water Investigation Directorate, Kolkata 700 091, India

In this study, one of the latest space-based techniques for measuring sub-centimetric ground displacement, Differential Synthetic Aperture Radar Interferometry (D-InSAR) has been used to assess the potential land subsidence phenomenon of Kolkata city, India. The occurrence of a thick surface clay layer with an average thickness of ~40 m and above, raises a question on the land subsidence phenomenon in Kolkata city. At this juncture, the D-InSAR-based study will help to ascertain the actual land subsidence scenario of Kolkata city. We have identified an area in Kolkata city in and around Machhua Bazar, Calcutta University and Raja Bazar Science College, which had been undergoing subsidence during the period of observation, i.e. 1992–98 with an estimated rate of 5 to 6.5 mm/yr.

Keywords: D-InSAR, land subsidence, Kolkata city.

PRESENTLY, Differential Synthetic Aperture Radar Interferometry (D-InSAR) has been found to be an efficient technique for measuring land subsidence in a number of studies[1–6]. D-InSAR is used for two broad purposes: (i) identification of land subsidence phenomenon in an area, and (ii) quantitative analysis and modelling of deformation phenomenon with particular emphasis on precision of measurements. In the latter case, the D-InSAR technique should be accompanied by precise GPS monitoring and/or ground-based levelling. In this study, an attempt has been made primarily to identify the subsiding areas in Kolkata city, India (Figure 1), and the approximate rate of subsidence during 1992–98. In Kolkata city, due to over-drafting of groundwater under confined aquifer condition, potential land subsidence phenomenon has been reported by a number of workers[7,8] and by the local media. In confined aquifer condition, over-extraction of groundwater causes lowering of piezometric pressure, which results in the development of tensional forces in overlying confining layer material. Consequently, compaction of overlying confining layer material takes place and land

*For correspondence. (e-mail: rschatterjee@iirs.gov.in)

subsidence occurs. In Kolkata city, presence of a thick surface clay layer with an average thickness of more than 40 m (up to 60–70 m at places) over the aquifer sand layer, raises a question on the possibility and doubtfulness of land subsidence. Under such circumstances, the D-InSAR-based study has the capability to assess actual land subsidence scenario of Kolkata city.

When two radar images are acquired at some time interval, the interferometric phase difference of the data pair is sensitive to topography of the terrain and any ground displacement that might have occurred during the data acquisition time interval. When topographic contribution to interferometric phase difference is known, the phase difference resulting from ground displacement can be obtained. However, variation in atmospheric conditions at the time of two data acquisitions and the temporal decorrelation between two images should be insignificant. Physiographically, Kolkata city and the surrounding areas represent a typical deltaic flat country[9], with elevation ranging between 5.8 and 6.1 m asl. The average building height in Kolkata city varies from 5 m (for single- or double-storeyed houses) to 15 m (for five-storeyed houses), excluding a few 10–20-storeyed high-rise buildings scattered in the city centre and newly developed commercial and residential clusters (near E.M. byepass). In case of ERS data pairs, for an average height variation of 10 m, there is a topographic phase contribution of 1/10, 1/20 and 1/50 fraction of a complete phase cycle (2π radians) for 100, 50 and 20 m spatial baseline pairs. Hence, topographic phase removal was not necessary in the present study area. For identifying slow subsidence in Kolkata city, we need to have InSAR data pairs with sufficiently large temporal baselines (generally in years), which introduces significant temporal decorrelation in the data pairs. Similarly, spatio-temporal variation of the atmospheric profile during acquisition of two images of an InSAR pair may contribute atmospheric artefacts in the interferograms. In slowly subsiding areas, as in Kolkata city, atmospheric fringes may appear comparable to deformation fringes. Filtering of the noisy interferograms and suppression of atmospheric artefacts from deformation fringes are crucial steps in this study for identifying the subsiding areas.

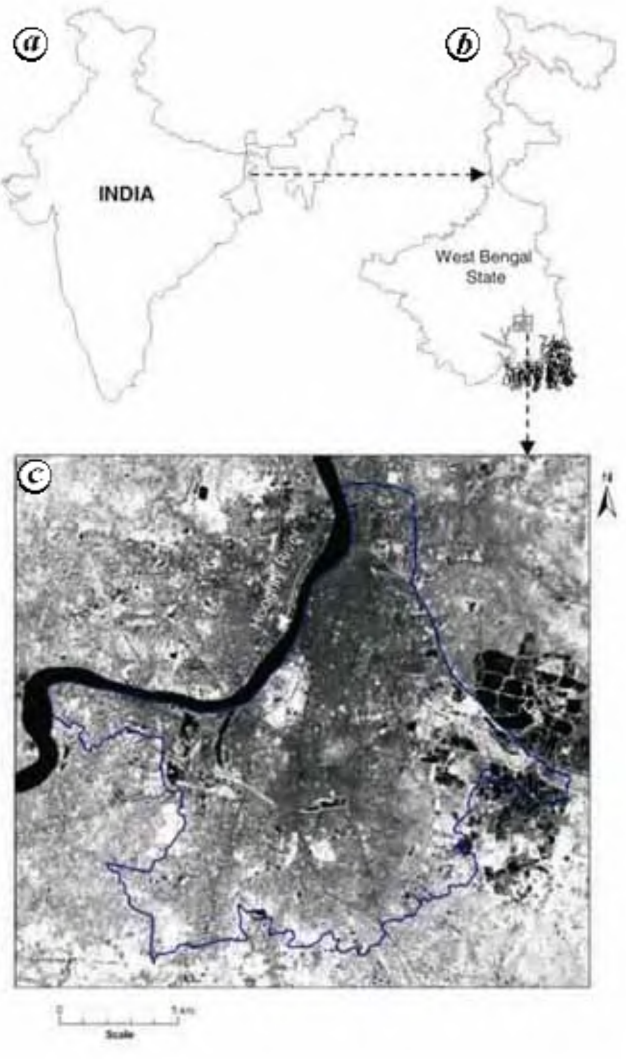

Figure 1. *a*, *b*, Location of Kolkata city, India. *c*, Landsat 5 TM near-infrared (NIR: 0.76–0.9 μm) image of Kolkata city and surrounding areas of 1998, where the study area, i.e. core city area under Kolkata Metropolitan Corporation is shown by the boundary line.

In a D-InSAR interferogram, a complete phase cycle (i.e. 2π radian phase difference) or fringe represents radar line-of-sight ground displacement of $\lambda/2$, where λ is the radar wavelength being used. For example, in case of C-band radar (λ = 5.6 cm), each fringe represents 2.8 cm or 28 mm radar line-of-sight displacement. As land subsidence movement is vertical in nature, the radar line-of-sight ground displacement can be converted into actual land subsidence by dividing the former value with cosine of radar incidence angle. In case of ERS satellites (ERS1 and ERS2) having C-band radar systems, the mean incidence angle is 23° and therefore, each fringe represents 28/cos(23°) or 30.42 mm of land subsidence.

In this study, four InSAR data pairs with master image (previous: t_1) acquired during post-monsoon time and the slave image (later: t_2) acquired during pre-monsoon time (Table 1) have been processed. During pre-monsoon time in a year, generally the piezometric head is low, whereas during post-monsoon time of the same year it is high. Two types of deformation can occur due to piezometric fall. The aquifer sand layer undergoes elastic compression as long as piezometric fall continues which, however, reverts when the piezometric head rises during post-monsoon. On the other hand, decrease in artesian pressure in the aquifer creates a hydraulic gradient between aquifer and overlying clay layer, which results in the leakage of pore water from the confining layer. The draining out of pore water from the clay layer reduces pore pressure and therefore, inelastic compression of the confining layer takes place. The piezometric fall is maximum during

Table 1. ERS1 and ERS2 InSAR data pairs of Kolkata city with post-monsoon (master: t_1) vs pre-monsoon (slave: t_2) combinations acquired during 1992–98

Interferogram	7335E1* 10.12.92	10842E1* 12.08.93	11343E1* 16.09.93	24713E1* 06.04.96	25214E1* 11.05.96	6543E2* 21.07.96	17064E2* 26.07.98	Remarks
'a'	←			$B_\perp$ = 14 m $B_\parallel$ = 11 m			→	Low to moderate coherence; fairly well-defined fringe(s)
'b'		←		$B_\perp$ = –131 m $B_\parallel$ = –79 m	→			Low to moderate coherence; fairly well-defined fringe(s)
'c'		←		$B_\perp$ = –35 m $B_\parallel$ = –36 m		→		Low coherence; poorly-defined fringe(s)
'd'			←	$B_\perp$ = –25 m $B_\parallel$ = 29 m	→			Low to moderate coherence; fairly well-defined fringe(s) with atmospheric artefacts

*E1 and E2 stand for ERS1 and ERS2 satellite missions and are followed by the respective orbit numbers.

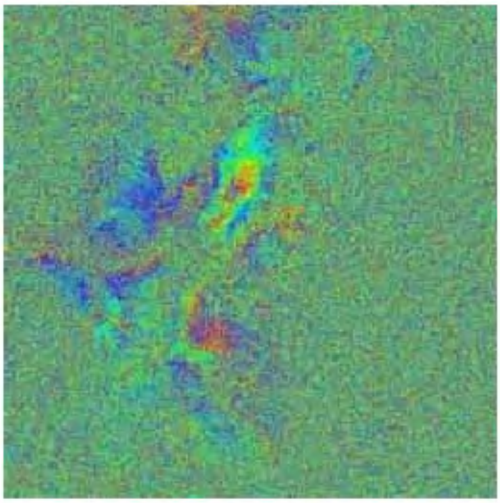

Interferogram 'a' = ERS1-7335 (10.12.92) and ERS2-17064 (16.07.98); ($B_\perp$ = 14 m; $B_\parallel$ = 11 m; Δt = 2044 days)

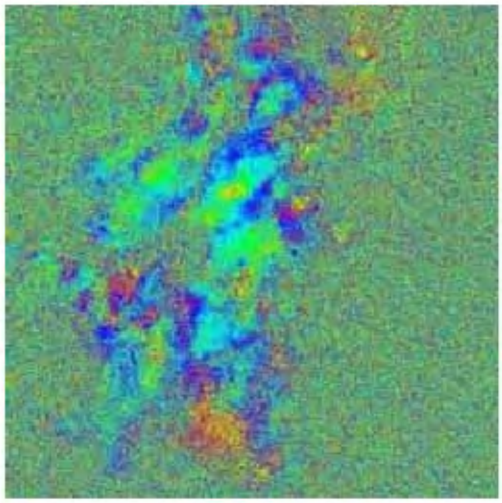

Interferogram 'b' = ERS1-10842 (12.08.93) and ERS1-24713 (06.04.96); ($B_\perp$ = –131 m; $B_\parallel$ = –79 m; Δt = 968 days)

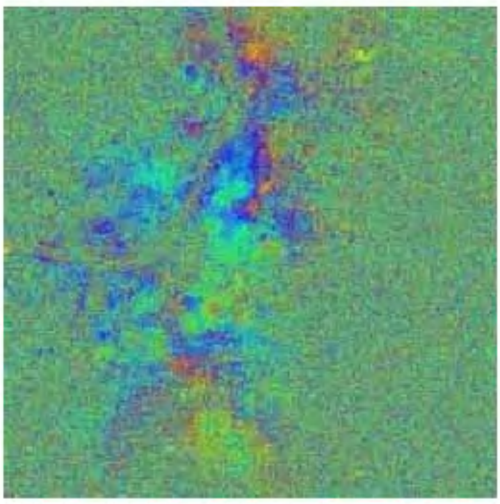

Interferogram 'c' = ERS1-10842 (12.08.93) and ERS2-6543 (21.07.96); ($B_\perp$ = –35 m; $B_\parallel$ = –36 m; Δt = 1074 days)

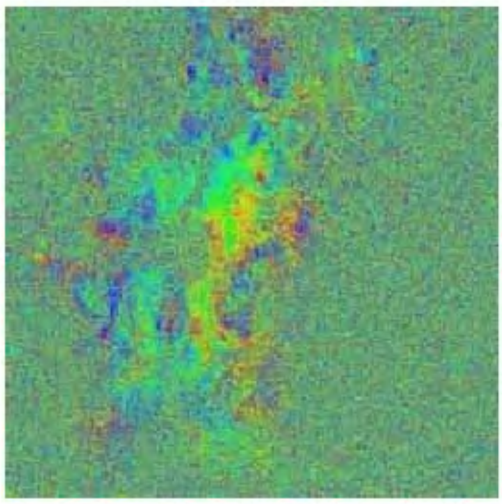

Interferogram 'd' = ERS1-11343 (16.09.93) and ERS1-25214 (11.05.96); ($B_\perp$ = –25 m; $B_\parallel$ = 29 m; Δt = 968 days)

Figure 2. Filtered interferograms 'a', 'b', 'c' and 'd' displayed in rainbow colour scheme showing several fringes (deformation fringes and atmospheric artefacts).

post-monsoon (t_1)–pre-monsoon (t_2) periods, which leads to both elastic compression of the aquifer and inelastic compression of the confining clay layer. The resulting land subsidence is, therefore, believed to be more pronounced in such cases compared to that in pre-monsoon (t_1)–pre-monsoon (t_2) and post-monsoon (t_1)–post-monsoon (t_2) periods of similar duration.

D-InSAR data processing was carried out using DIAPASON software developed by the French Space Agency (CNES). Temporal decorrelation in the data pairs and atmospheric effects have been found to pose serious difficulties in identifying and separating the deformation fringes. Filtering of noisy interferograms was carried out using the adaptive filter of Goldstein and Werner[10]. Subsequently, summing up the filtered interferograms was accomplished in complex domain to highlight the deformation fringes and to dilute the atmospheric artefacts, as atmospheric phase contribution is spatio-temporally random in nature. The detailed procedure is available in Chatterjee *et al.*[11].

It is observed that in interferograms 'a', 'b' and 'd' (i.e. ERS1_7335 vs ERS2_17064, ERS1_10842 vs ERS1_24713 and ERS1_11343 vs ERS1_25214 respectively), coherence is low to moderate and fringe(s) are fairly well-developed. In interferogram 'c' (i.e., ERS1_10842 vs ERS2_6543), coherence is low and the fringe(s) are poorly developed.

Initially, the interferograms were studied individually to find out fringe(s) with common geographic location in different interferograms, so that fringe(s) representing land subsidence can be separated from atmospheric artefacts. It is known that spatial variability of the atmosphere with time and therefore fringes produced by atmospheric effects do not lie normally at constant geographic position in independent interferometric pairs, whereas land subsidence may continue to occur at the same locations for a period of time due to similar prevailing conditions responsible for land subsidence. We have observed a poorly to fairly well-defined fringe with common geographic location in the interferograms after filtering (interferograms 'a', 'b', 'c' and 'd', Figure 2). Subsequently, the independent interferograms 'a' and 'b', and 'b' and 'd' have been summed-up separately in complex domain to highlight deformation fringes over atmospheric artefacts (Figure 3). In the sum interferograms, a well-defined deformation fringe has been observed. Assuming a simplified linear uniform subsidence over time, the average rate of land subsidence has been measured separately from two sum interferograms. From the sum interferograms 'ab' and 'bd', the rate of land subsidence has been found to range between 5 and 6.5 mm/yr (maximum). Both the sum interferograms were then displayed in IHS colour space using sum interferometric phase as hue component, coherence image of one of the interferometric pairs of the sum interferogram (preferably the better coherence image) as saturation component and average amplitude image of one of the interferometric pairs of the sum interferogram as intensity component (Figure 4). In IHS images of sum interferograms, it is observed that the subsidence fringe is located in and around Machhua Bazar, Calcutta University and Rajabazar Science College.

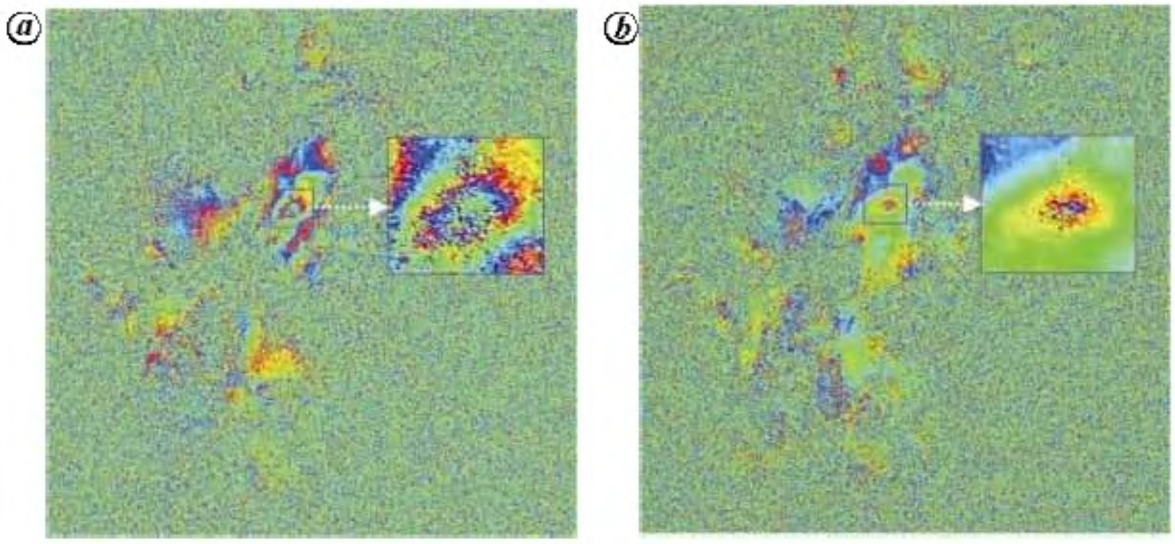

Interferogram 'a' = ERS1-7335 (10.12.92) and ERS2-17064 (16.07.98); Δt = 2044 days
Interferogram 'b' = ERS1-10842 (12.08.93) and ERS1-24713 (06.04.96); Δt = 968 days

Interferogram 'b' = ERS1-10842 (12.08.93) and ERS1-24713 (06.04.96); Δt = 968 days
Interferogram 'd' = ERS1-11343 (16.09.93) and ERS1-25214 (11.05.96); Δt = 968 days

Figure 3. Sum-interferograms of 'a' and 'b' individual interferograms (***a***) and 'b' and 'd' individual interferograms (***b***) respectively. Deformation rate may be obtained by dividing total deformation with total time interval elapsed by two individual interferograms (in either case assuming uniform deformation).

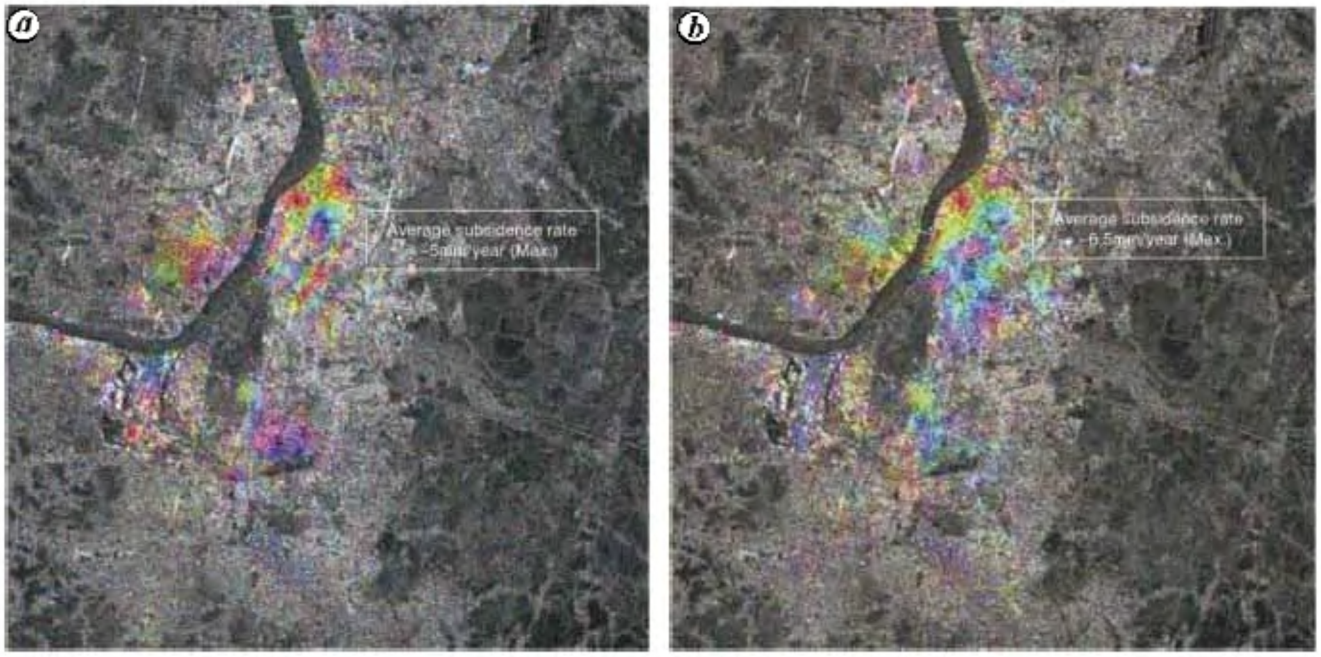

Phase image of sum-interferogram 'ab' as hue (H), average amplitude image of the interferogram 'b' as intensity (I) and coherence image of the interferogram 'b' as saturation (S) components in IHS image display.

Phase image of sum-interferogram 'bd' as hue (H), average amplitude image of interferogram 'b' as intensity (I) and coherence image of interferogram 'b' as saturation (S) components in IHS image display.

Figure 4. IHS colour composition of sum-interferograms (H) ((***a***) and (***b***) respectively, as in Figure 3), average backscattered amplitude image of one of the interferograms of the sum interferogram (I) and coherence image of one of the interferograms of the sum interferogram (S) to highlight the areas that underwent subsidence during the 1990s.

The present study describes the subsidence scenario of Kolkata city during 1992–98 from the available InSAR data pairs. However, due to lack of sufficient temporal correlation in InSAR data pairs over the entire city area, it is difficult to negate definitively if any other area of Kolkata city underwent subsidence during the study period, i.e. 1992–98. Moreover, it is important to separate the inelastic component of total deformation for each year for measuring total permanent deformation during the study period. More InSAR data pairs with reasonable coherence and dense temporal intervals are required to address the above problems.

Now, it is important to assess the present subsidence scenario of Kolkata city and to study the spatio-temporal evolution of subsidence during last few years. The results obtained from D-InSAR technique may be accompanied by precise GPS monitoring and ground-levelling measurements for validation. It is encouraging to note here that West Bengal State Water Investigation Directorate has taken up a number of measures to maintain piezometric level in Kolkata city during the last few years, e.g. artificial recharge, rainwater harvesting which will reduce the subsidence threat in Kolkata city substantially.

1. Amelung, F., Galloway, D. L., Bell, J. W., Zebker, H. A. and Laczniak, R. J., Sensing the ups and downs of Las Vegas: InSAR reveals structural control of land subsidence and aquifer system deformation. *Geology*, 1999, **27**, 483–486.
2. Fruneau, B. and Sarti, F., Detection of ground subsidence in the city of Paris using radar interferometry: Isolation from atmospheric artefacts using correlation. *Geophys. Res. Lett.*, 2000, **27**, 3981–3984.
3. Tesauro, M., Beradino, P., Lanari, R., Sansoti, E., Fornaro, G. and Franceschetti, G., Urban subsidence inside the city of Napoli (Italy) observed by satellite radar interferometry. *Geophys. Res. Lett.*, 2000, **27**, 1961.
4. Strozzi, T., Wegmüller, U., Tosi, L., Bitelli, G. and Spreckels, V., Land subsidence monitoring with differential SAR interferometry. *Photogramm. Eng. Remote Sensing*, 2001, **67**, 1261–1270.
5. Crosetto, M., Tscherning, C. C., Crippa, B. and Castillo, M., Subsidence monitoring using SAR interferometry: Reduction of the atmospheric effects using stochastic filtering. *Geophys. Res. Lett.*, 2002, **29**, 26-1–26-4.
6. Ding, X. L., Liu, G. X., Li, Z. W., Li, Z. L. and Chen, Y. Q., Ground subsidence monitoring in Hong Kong with satellite SAR interferometry. *Photogramm. Eng. Remote Sensing*, 2004, **70**, 1151–1156.
7. Biswas, A. B. and Saha, A. K., Environmental hazards of the recession of piezometric surface of groundwater under Calcutta. *Proc. Indian Natl. Sci. Acad. Part A*, 1985, **51**, 610–621.
8. Sikdar, P. K., Biswas, A. B. and Saha, A. K., A study on the possible land subsidence in Calcutta and Howrah cities due to groundwater overdraft. *Indian J. Geol.*, 1996, **68**, 193–200.
9. Chaterji, G. C., Biswas, A. B., Basu, S. and Niyogi, B. N., Geology and groundwater resources of Greater Calcutta industrial area, West Bengal. *Bull. Geol. Surv. India, Ser. B*, 1964, **21**, 1–67.
10. Goldstein, R. and Werner, C., Radar interferogram filtering for geophysical application. *Geophys. Res. Lett.*, 1998, **25**, 4035–4038.

11. Chatterjee, R. S. *et al.*, Subsidence of Kolkata (Calcutta) city, India during the 1990s as observed from space by Differential Synthetic Aperture Radar Interferometry (D-InSAR) technique. *Remote Sensing Environ.*, 2006, **102**, 176–185.

ACKNOWLEDGEMENTS. The work has been carried out under ESA Category-1 project in collaboration with Institut Francilien des Geosciences (IFG), Université de Marne-la-Vallée (UMLV), France. We acknowledge technical assistance and contribution from Prof. Jean-Paul Rudant, Dr Benedicte Fruneau and Dr Pierre-Louis Frison, IFG, UMLV, France. We thank the European Space Agency for providing ERS SAR data at reproduction cost. We also thank the Central Ground Water Board (Kolkata), State Water Investigation Directorate (West Bengal), Metro Rail (Kolkata) and National Atlas and Thematic Mapping Organization (Kolkata) for providing collateral data and ancillary information.

We are grateful to the anonymous reviewers for their analytical remarks and critical comments on the manuscript.

Received 23 January 2006; revised accepted 19 February 2007

Chronology of the Late Quaternary glaciation around Badrinath (Upper Alaknanda Basin): Preliminary observations

H. C. Nainwal[1,*], M. Chaudhary[1], N. Rana[1], B. D. S. Negi[1], R. S. Negi[1], N. Juyal[2] and A. K. Singhvi[2]

[1]Department of Geology, HNB Garhwal University, Srinagar (Garhwal) 246 174, India
[2]Physical Research Laboratory, Navrangpura, Ahmedabad 380 009, India

Reconstruction based on the presence of lateral moraines and other relict periglacial features in Upper Alaknanda basin indicates three phases of glaciation during the Late Quaternary. From oldest to youngest, they are named as Alaknanda (Stage-I), Alkapuri (Stage-II) and Satopanth (Stage-III) glacial advances. The oldest Stage-I was the most extensive glaciation in the basin that reached south of Badrinath (2604 m asl). Compared to this, the other two glaciations were terminated around 3550 and 3700 m asl respectively, in the N–S trending Upper Alaknanda basin. Preliminary estimate based on limited optical dating suggests the Stage-I predates the Last Glacial Maximum (LGM). An indirect age estimate based on the chronology of recessional moraine dated to 12 ka suggests that Stage-II was deposited during the LGM whereas Stage-III is dated to 4.5 ka. Conical heaps in the vicinity of the present-day snout are attributed to the recent recession probably associated with the Little Ice Age.

*For correspondence. (e-mail: nainwalhc@yahoo.co.in)

Keywords: Late Quaternary glaciations, optical dating, periglacial features, Satopanth and Bhagirath Kharak glaciers.

THE seasonal distribution of precipitation in Himalayan glaciers is of summer accumulation-type, i.e. maximum accumulation and ablation occurs during summer[1,2]. Towards the growth of the glaciers, the Indian Summer Monsoon (ISM) is a major source of moisture[3]. Hence changes in the extent of valley glaciers can be used to reconstruct the past precipitation and temperature conditions. These changes are manifested in the pattern of distribution of the glacial sediments, particularly the lateral moraines. In a valley glacier, the highest point of lateral moraines coincides with the Equilibrium Line Altitude and terminates at the snout[4].

In the Trans-Himalayan region, evidence for past glaciations is preserved in the form of well-developed moraines and valley fills that exceed several tens of metres in thickness. According to Owen *et al.*[5], the extent of valley glaciations varied considerably throughout the Late Quaternary. Although most studies indicate multiple events of glaciation in the Himalaya, quantitative estimate on their timing is lacking due to scarcity of organic material that precludes the use of standard radiocarbon-dating techniques. Recent advancement in luminescence dating has opened up the possibility of proving the timing of the Late Quaternary in the region[3]. There exists some estimate on the timing of various glacial advancements from the Central Himalaya[6,7], which provides insight into the fluctuations in ISM during the Late Quaternary. This study is a contribution towards understanding the magnitude and variability in the Late Quaternary glaciation in the Upper Alaknanda basin, in which an attempt has been made to reconstruct the pattern of glaciation. Lateral moraines associated with three glacial advances are well preserved in the Upper Alaknanda basin. These are named as Alaknanda (Stage-I), Alkapuri (Stage-II) and Satopanth (Stage-III) glacial advances. In order to reconstruct the stratigraphy of various glacial advancements and related glaciogenic features, field mapping was carried out at 1 : 50,000 scale supported by Total Station (TS) survey. It was found that Stage-I glaciation was the most extensive that reached south of Badrinath (3000 m asl), whereas the successive glacial advances, viz. Stages-II and III were restricted around 3550 and 3700 m asl respectively. Further, in order to ascertain the timing of various glacial stages, a preliminary chronology using the Optical Stimulated Luminescence dating techniques on lateral moraine and glacio-fluvial sediments has been attempted.

Lithology of the area is dominated by calc-silicate, boitite gneiss, schist and granite (pegmatite–apatite veins) belonging to the Pindari Formation[8]. A regionally extensive Pindari Thrust that passes through Hanuman Chatti is a major structural feature that differentiates two distinct basins, the wide U-shaped Badrinath basin from the narrow V-shaped Pandukeshwar basin.